Sensitivity tests on parameters of the nucleon-nucleus dispersive optical model

G. J. Weisel and R. L. Walter
Department of Physics and Triangle Universities Nuclear Laboratory, Duke University, Durham, North Carolina 27708
(Received 11 August 1998)

We have conducted tests of two changes to the formalism of the dispersive optical model (DOM) by making use of a large $n+^{208}$Pb database. One change relaxes the constraint, conventional in DOMs, that the real- and imaginary-volume potentials share the same geometrical parameters. The second change adopts a different functional form for the energy dependence of the surface imaginary potential, which allows its strength to drop off rapidly in the 30–80 MeV region. Radial shapes of the total imaginary potentials for the new DOMs are compared to each other and to those of a microscopic optical model. We also present an improved DOM analysis which models elastic scattering data for $n+^{208}$Pb and $n+^{209}$Bi simultaneously, and which incorporates a newer set of $n+^{208}$Pb total cross-section data. [S0556-2813(99)06101-4]

PACS number(s): 24.10.Ht, 25.40.Dn, 28.20.Cz

For the past decade, the Triangle Universities Nuclear Laboratory (TUNL) has investigated the dispersive optical model (DOM), an optical model formalism that incorporates a dispersion relation linking the real and imaginary parts of the nuclear potential [1]. TUNL has applied the DOM to a number of neutron-nucleus scattering systems and has written software that optimizes the quality of fit of the DOM predictions to the data, as measured by the so-called chi-squared [2]. In the course of this work, questions have arisen about two aspects of the DOM formalism. The first is the constraint, found in all DOM analyses using Woods-Saxon form factors, that the real- and imaginary-volume potentials share the same geometrical parameters. Since traditional optical models have found that fits to data favor a radius for the volume imaginary potential that is four to six percent larger than that for the volume real potential, we suspected that incorporating such a difference might improve the quality of fit for the DOM approach. The second constraint concerns the functional form of the energy dependence of the surface imaginary potential $W_s(E)$. In past work, the form we used [Eq. (3), below, with $j=1$] favored relatively large values for $W_s(E)$ at high incident neutron energies (30–80 MeV), as compared to traditional optical models. This motivated us to switch to a revised form for $W_s(E)$, which would reduce its value at high energies but not worsen the overall fits. As one might anticipate, these two aspects of the formalism are related; the relative strengths of the imaginary potentials are affected both by changing the radius of the volume imaginary potential and by altering the functional form of the energy dependence of the surface imaginary potential.

We decided to use an $n+^{208}$Pb DOM for the present sensitivity tests, since we had experience with this scattering system from work on a unified DOM analysis of $n+^{208}$Pb and $n+^{209}$Bi from -20 to $+80$ MeV [2,3]. The objective of that study was to fit the ^{208}Pb and ^{209}Bi data bases by using as many common parameters as possible. In the final stages of the DOM searches, we found it easy to compromise between the two scattering systems for the parameters of the volume-imaginary potential, but difficult for those of the surface-imaginary potential. As Ref. [2] points out, this was due to differences in the high-energy regime between the total cross-section data for the two systems. The $n+^{208}$Pb data in the 50–80 MeV range, from Shutt *et al.* [4], was systematically higher than the $n+^{209}$Bi data, from Finlay *et al.* [5], by about one and a half percent. As a result of this, the ''partially constrained'' ^{208}Pb and ^{209}Bi DOMs of Ref. [2] had considerably different slope factors for $W_s(E)$, of $C_s=0.0128$ and $C_s=0.0197$, respectively. The low value of C_s for ^{208}Pb corresponds to relatively large values of $W_s(E)$ at high energies.

Since newer $n+^{208}$Pb total cross-section data is available from Ref. [5], we tried using it in place of the data of Ref. [4] in the present work. To create a new unified ^{208}Pb-^{209}Bi DOM, we started with the parameters for the ''partially constrained'' ^{209}Bi DOM of Ref. [2], and retuned only the five strength parameters of the imaginary potentials. We found that the $W_s(E)$ parameters of the ^{208}Pb DOM now favored values within 5% of those for ^{209}Bi, thus eliminating the need for two separate partially constrained DOMs. The parameters of the new unified ^{208}Pb-^{209}Bi DOM are the same as those appearing in the ''w/W_{so}'' column of Ref. [2], except for the following differences: $A_v=5.87$, $B_v=29.32$, $A_s=9.95$, $B_s=4.91$, and $C_s=0.0200$. Note that the model uses a significantly larger C_s value than the partially constrained ^{208}Pb DOM of Ref. [2]. Figure 1 displays the $n+^{209}$Bi and $n+^{208}$Pb total cross-section data of Ref. [5], along with the predictions of the new unified DOM. The model's predictions for differential scattering data and for bound-state quantities are similar to those of Ref. [2] and so are not shown.

In preparation for the sensitivity studies, we started with the new unified DOM and optimized the quality of fit to the ^{208}Pb data alone by fine-tuning all of the DOM parameters, except for the spin-orbit parameters and the slope of the Hartree-Fock (HF) field B_{HF}. (Maintaining $B_{HF}=0.0350$ was best for the prediction of single-particle binding energies.) We refer to this standard model as DOM I.

In conventional optical model analyses, optimization of the fit to data usually requires that the radius of the volume imaginary potential be made four to six percent greater than the radius of the real potential. In contrast to this, all published DOMs have constrained the HF potential and volume imaginary potential to share the same geometrical param-

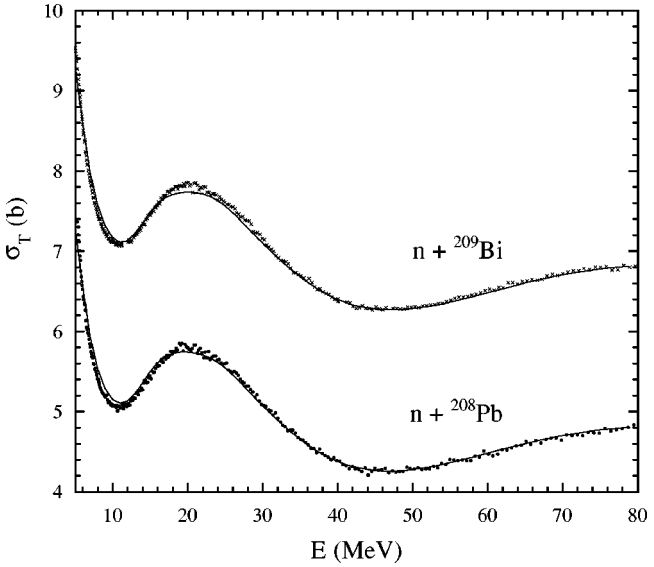

FIG. 1. Total cross-section data [5] compared to predictions of the new unified ^{208}Pb-^{209}Bi DOM. The offset is 2 b for ^{209}Bi.

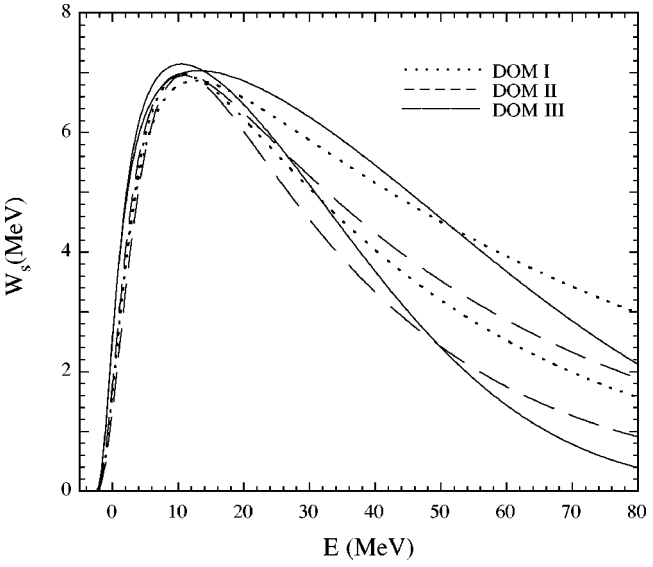

FIG. 2. Bands of $W_s(E)$ corresponding to a chi-squared tolerance of 2% for DOM I, DOM II, and DOM III.

eters. This assumption has been made largely for convenience. Recall that the DOM approach links the volume imaginary potential to a ''dispersive correction'' $\Delta V_v(r,E)$ to the volume real potential through an integral relation. If the Hartree-Fock and volume imaginary potentials share the same geometry, then the total volume real potential is determined simply by adding the strengths of the HF potential and the volume dispersive correction, and multiplying the sum by a common geometrical form factor [2,6]:

$$V_v(r,E)=[V_{\rm HF}(E)+\Delta V_v(E)]f_{\rm WS}(r,R_v,a_v). \qquad (1)$$

The $f_{\rm WS}(r,R_v,a_v)$ is a Woods-Saxon form factor, where the nuclear radius R_v is written in terms of the parameter r_v and the total mass number as $R_v=r_vA^{1/3}$. In our first set of sensitivity tests, we relaxed the constraint posed by Eq. (1) by using a total volume real potential of the form:

$$V_v(r,E)=V_{\rm HF}(E)f_{\rm WS}(r,R_{\rm HF},a_{\rm HF})+\Delta V_v(E)f_{\rm WS}(r,R_v,a_v). \qquad (2)$$

We refer to a model incorporating Eq. (2) as a DOM II.

In our tests, we held the radius $r_{\rm HF}$ of the HF field constant while increasing the radius r_v of the volume imaginary potential in 0.01 fm steps. We also maintained a constant difference between $r_{\rm HF}$ and r_v, and stepped their values in unison, e.g., $r_{\rm HF}/r_v=1.22/1.27,1.23/1.28$, etc. For each pairing, the other DOM parameters were reoptimized for the chi-squared quality of fit to the data, except for the spin-orbit parameters and $B_{\rm HF}$. None of the DOM IIs demonstrated better fits to the data. Though failing in its primary objective, this modification had an effect on the strength parameters that is worth noting. As r_v became closer to the radius r_s of the surface imaginary potential, the trade off between the W_v and W_s strengths was altered such that $W_s(E)$ could be made smaller-valued at high energies. While DOM I gave a W_s strength as high as 3.0 MeV at $E=80$ MeV, DOM II, using $r_{\rm HF}/r_v=1.23/1.28$, gave a maximum strength of 1.9 MeV (as can be seen in Fig. 2, discussed below).

Although DOM II introduces a satisfying change to the W_s energy dependence, it does not improve fits to the data and introduces two new parameters, $r_{\rm HF}$ and $a_{\rm HF}$. In an attempt to maintain the difference between $r_{\rm HF}$ and r_v, but eliminate two degrees of freedom, we forced $r_v=r_s$ and $a_v=a_s$, as in traditional (non-DOM) optical models. Because the chi-squared searches always yielded relatively large values for a_v and small values for a_s (roughly 0.680 and 0.500, respectively), attempting to compromise to a single value resulted in a worse fit to the data (chi-squared increased by 20%). We conclude that allowing the radius of the volume-imaginary potential to be greater than that of the volume-real potential is not favorable for a DOM of $n+^{208}$Pb.

The most obvious way of affecting the behavior of the surface imaginary potential at high energy is to change the functional form of its energy dependence. Consider the fol-

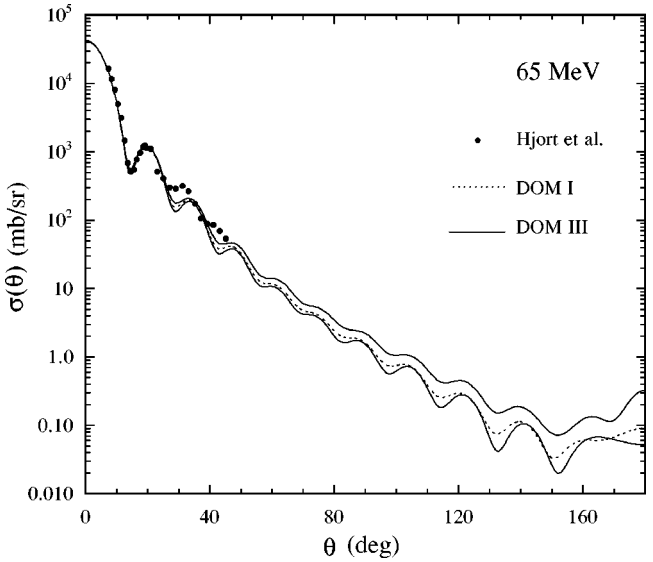

FIG. 3. Cross-section data at 65 MeV for $n+^{208}$Pb [8] compared to predictions of DOM III, within a 2% chi-squared tolerance, and DOM I, for the optimum solution only.

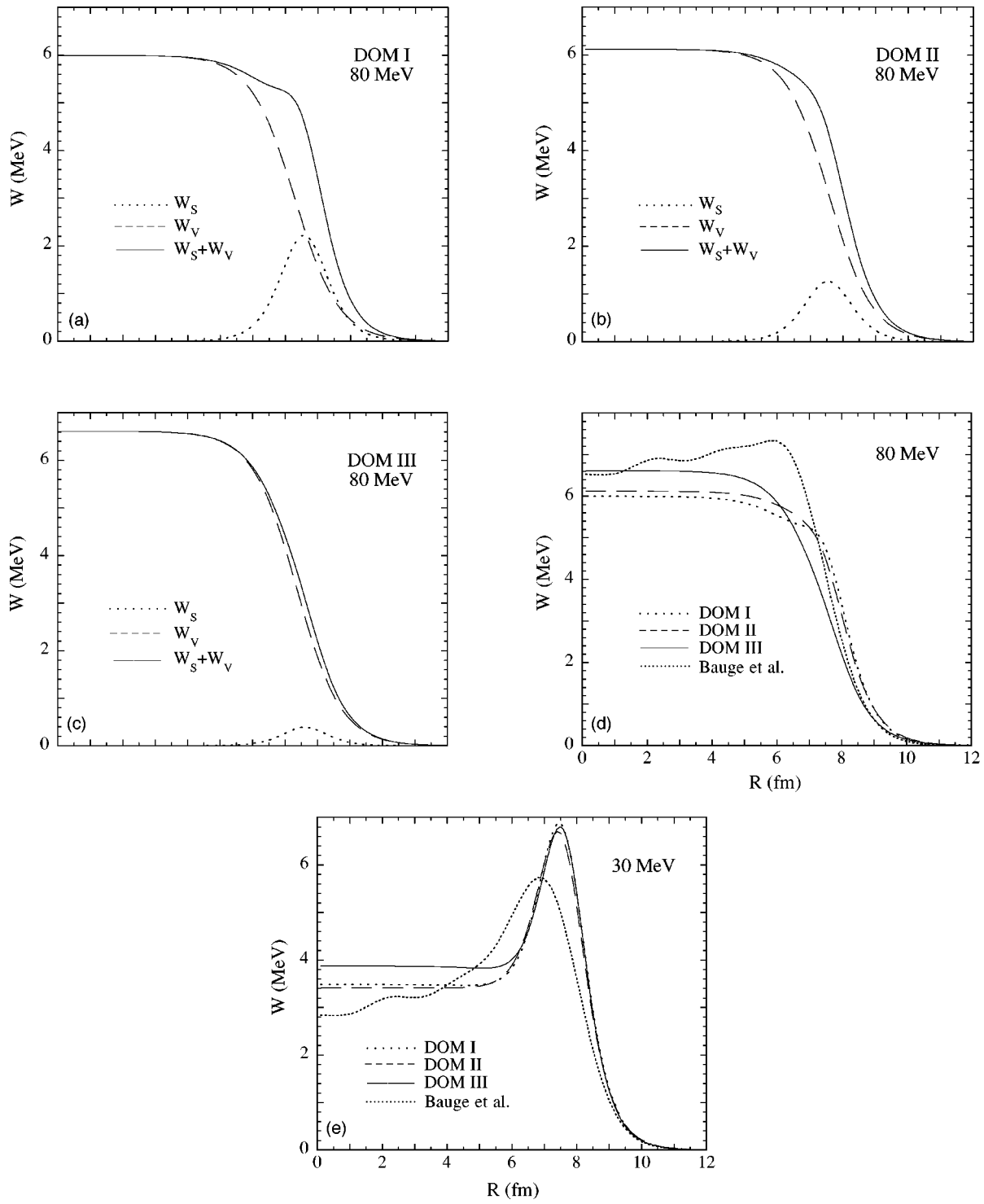

FIG. 4. The $W(r)$ for the optimum DOM I and DOM II, and DOM III with the maximum value for C_s, compared to that for the microscopic optical model of Ref. [9] at 30 and 80 MeV. At 80 MeV, $W_v(r)$ and $W_s(r)$ are also displayed.

lowing form for $W_s(E)$, which is parametrized about the Fermi energy E_F and contains an undetermined power j. For $E > E_p$, where E_p is the average energy of the single-particle bound states,

$$W_s(E) = \frac{A_s(E-E_p)^2}{(E-E_p)^2+B_s^2}\exp[-C_s(E-E_p)^j] \qquad (3)$$

and for $E_F \leqslant E \leqslant E_p$, $W_s(E)=0$. The $W_s(E)$ is an even function with respect to E_F. In all of TUNL's past DOM analyses using Eq. (3), we set $j=1$ and found that fits to the data favored values for C_s that made $W_s(E)$ relatively large at high incident neutron energies. While conventional optical models usually allow the strength of the surface imaginary potential to go to zero by $E=80$ MeV, our DOMs had strengths for $W_s(E)$ as high as 3.2 MeV at $E=80$ MeV, corresponding to values of C_s as low as 0.0108 MeV^{-1} [2,7]. In the present sensitivity tests, we stepped the value of C_s in 0.0010 increments, retuned the other DOM parameters, and noted the effect that this had on chi-squared. Within a

2% deviation of chi-squared from its minimum value, DOM I favored C_s values in the range 0.0190 ± 0.0050 (optimum solution: $A_s = 10.39$, $B_s = 5.40$, $C_s = 0.0190$). Higher C_s values are possible with DOM II, which favored the range 0.0270 ± 0.0060 (optimum solution: $A_s = 12.16$, $B_s = 6.19$, $C_s = 0.0270$). It should be noted that, because $B_{\rm HF}$ was not altered, the predictions to bound-state quantitites did not change significantly. For example, the high end of the C_s variation yielded relatively low magnitudes for the strength $A_{\rm HF}$ of the HF field which resulted in the single-particle states being underbound by roughly 100 keV.

To determine how low the magnitude of $W_s(E)$ at 80 MeV could be forced, our second set of sensitivity tests adopted Eq. (3) with $j = 2$. We refer to a model using Eq. (3) with $j = 2$ as a DOM III. For each C_s value, all other DOM parameters were tuned except for the spin-orbit parameters and $B_{\rm HF}$. Within a chi-squared tolerance of 2%, the resulting parameter sets favored values of C_s in the range $(0.0320 \pm 0.0130) \times 10^{-2}$ MeV^{-2} (optimum solution: $A_s = 7.93$, $B_s = 3.36$, $C_s = 0.0320 \times 10^{-2}$). DOM III did not improve the fits to the data. Figure 2 shows bands of $W_s(E)$ for our three models using the favored ranges of C_s values: DOM I (dotted lines), DOM II (using $r_{\rm HF}/r_v = 1.23/1.28$) (dashed), and DOM III (solid).

In attempting to determine which of these energy dependencies is preferable, we found it impossible to make use of a qualitative or quantitative judgement of the quality of fits to the data; all of the models under consideration gave fits that were nearly identical from visual inspection and had chi-squared values within 4% of one another. Two scattering observables which are sensitive to the high-energy behavior of $W_s(E)$ are differential cross section and analyzing power at high incident neutron energies ($E > 40$ MeV) and large angles ($\theta > 60°$). However, none of the available ^{208}Pb(n,n) differential cross-section data above 40 MeV has been taken at large angles. For example, the 65 MeV data of Hjort *et al.* [8] does not go beyond $\theta = 45°$. Figure 3 displays this data with the predictions of the optimum DOM I and two versions of DOM III using the lowest and highest favored values for C_s. Note, in the $60°$–$90°$ region, that the two limiting cases of DOM III yield differential cross-section predictions in the 1–10 mb/sr range that differ by 30%.

Figure 4 displays, at $E = 30$ and 80 MeV, the radial shapes of the total imaginary potential $W(r)$ for our three test DOMs, compared to those of the microscopic optical model of Bauge *et al.* [9]. For DOM I and DOM II, the optimum solutions are displayed ($C_s = 0.0190$, and 0.0270, respectively). To demonstrate the ability of DOM III to minimize the strength of the surface imaginary potential at high energies, the maximum favored value of C_s was used (0.0450×10^{-2}). At 80 MeV, $W_v(r)$ and $W_s(r)$ are also graphed in order to display their relative contributions. Note that the $W_s(r)$ for DOM III is much smaller than that for DOM I. Compared to the microscopic optical potential of Ref. [9], the $W(r)$ shapes for the three DOMs have somewhat smaller volume integrals at 80 MeV but somewhat larger volume integrals at 30 MeV. Because the $W(r)$ shapes for our DOMs and that for the microscopic optical model are qualitatively different, such comparisons cannot answer our questions regarding $W_s(E)$.

In summary, we revised the unified ^{208}Pb-^{209}Bi DOM of Ref. [2] by using the most recent total cross-section data. We also presented two sensitivity tests of the DOM formalism, using a model for $n + ^{208}$Pb up to 80 MeV (DOM I). When the radius of the imaginary volume potential is allowed to be 5% greater than that of the HF field (DOM II) the quality of fit to data is not improved. However, the alteration does make it possible to lower the strength of the surface imaginary potential at high energies. When the functional form of $W_s(E)$ is altered [using Eq. (3) with $j = 2$], it is possible to obtain low $W_s(E)$ values at large energies (DOM III). However, this alteration does not improve the quality of fit to the data. The DOM I and its two variations all have chi-squared fits to data that lie within 4% of each other. When differential cross-section data in the high energy (>40 MeV), high angle ($>60°$) regime become available, it will be possible to place stronger constraints on the energy dependence of $W_s(E)$ in the 30–80 MeV range.

The authors are grateful to E. Bauge for providing graphs of his optical-model potentials. This work was supported by the U.S. Department of Energy, Office of High Energy and Nuclear Physics, under Grant No. DEFG05-ER40619 with Duke University.

[1] C. Mahaux and R. Sartor, Adv. Nucl. Phys. **20**, 1 (1991).
[2] G. J. Weisel, W. Tornow, C. R. Howell, P. D. Felsher, M. Alohali, M. L. Roberts, R. K. Das, R. L. Walter, and G. Mertens, Phys. Rev. C **54**, 2410 (1996).
[3] G. J. Weisel, PhD dissertation, Duke University, 1992.
[4] R. L. Schutt, R. E. Shamu, P. W. Lisowski, M. S. Moore, and G. L. Morgan, Phys. Lett. B **203**, 22 (1988).
[5] R. W. Finlay, W. P. Abfalterer, G. Fink, E. Montei, T. Adami, P. W. Lisowski, G. L. Morgan, and R. C. Haight, Phys. Rev. C **47**, 237 (1993).
[6] C. H. Johnson, D. J. Horen, and C. Mahaux, Phys. Rev. C **36**, 2252 (1987).
[7] M. M. Nagadi, Ph.D. dissertation, Duke University, 1992.
[8] E. L. Hjort, F. P. Brady, J. L. Romero, J. R. Drummond, D. S. Sorenson, J. H. Osborne, B. McEachern, and L. F. Hansen, Phys. Rev. C **50**, 275 (1994).
[9] E. Bauge, J. P. Delaroche, and M. Girod, Phys. Rev. C **58**, 1118 (1998).